Zero Dynamics in Robotic Systems

ALESSANDRO DE LUCA

Abstract. *The notion of zero dynamics of a nonlinear system is used in the investigation of three classes of problems that arise in advanced robotics: control of robots in rigid contact with the environment, free motion control of manipulators with redundant degrees of freedom, and trajectory control of robot arms with flexible links. In each case, the internal dynamics present in the system when a proper output is constrained to be zero is characterized, and a physical interpretation of such dynamics is provided. Simple examples are worked out to show how this analysis supports the design of stabilizing controllers, and that existing results can be reviewed in the spirit of zero dynamics.*

1. Introduction

In recent years robotics has served as an exciting field of application for advanced findings in nonlinear control theory. Several interesting control problems have been posed and solved for nonlinear systems which are linear in the control input u and in the disturbance input z,

$$(1) \qquad \dot{x} = f(x) + g(x)u + r(x)z, \qquad y = h(x),$$

where $x \in \mathbb{R}^n$, $u \in \mathbb{R}^m$, $z \in \mathbb{R}^\ell$, $y \in \mathbb{R}^p$, f and the columns g_i and r_i of matrices g and r are smooth vector fields, and h is a smooth output vector function. In particular, necessary and sufficient conditions have been found for the problems of feedback linearization, input-output noninteraction, disturbance decoupling, and full (i.e. state plus output) linearization, using a static state-feedback law of the form

$$(2) \qquad u = \alpha(x) + \beta(x)v, \qquad \text{with } \beta(x) \text{ nonsingular,}$$

as control input and, when needed, a transformation in the state-space $\tilde{x} = \Psi(x)$ (see [1], and the references therein).

This general framework is well suited to robotics, as to many other mechatronics systems, for two main reasons. First, dynamic models of

articulated manipulators present strong, although smooth, nonlinearities in the state, but are always linear in the inputs. Mechanical sources of nonlinear dynamics are the large changes of apparent inertia in different arm postures and the dependency of gravity forces on the configuration. Second, in standard robot control problems, the relation between applied input forces and controlled outputs — the joint variables or the end-effector pose — fully displays the typical interactions of multivariable systems.

To set up a common background, let us recast some standard results for *conventional* robots, namely those manipulators constituted by open kinematic chains of rigid bodies, connected by N rotational or prismatic joints, and with an independent actuator driving each degree of freedom. Also, N is less or equal to 6, the maximum number of parameters needed for specifying an arbitrary position and orientation of the end-effector in free space. Defining a vector $q \in \mathbb{R}^N$ of generalized coordinates (e.g. the joint variables), the Lagrangian of the system $L = T - U + m^T q$, is formed from the kinetic energy $T(q, \dot{q}) = \frac{1}{2}\dot{q}^T B(q)\dot{q}$, the potential energy $U(q)$, and the nonconservative forces m performing work on q. Applying the principle of least action [2], the equations of motion for conventional robots are obtained as

$$(3) \qquad B(q)\ddot{q} + c(q, \dot{q}) + e(q) = m,$$

where B is the positive definite symmetric inertia matrix, c is the Coriolis and centrifugal vector, and e is the gravitational vector. The components of the last two terms have the explicit expressions

$$(4) \qquad c_i(q, \dot{q}) = \frac{1}{2}\dot{q}^T \left(\frac{\partial b_i}{\partial q} + \left(\frac{\partial b_i}{\partial q}\right)^T - \frac{\partial B}{\partial q_i}\right)\dot{q}, \qquad e_i(q) = \frac{\partial U}{\partial q_i},$$

for $i = 1, \ldots, N$, being b_i the ith column of B. State equations in the form (1) (with $z = 0$, viz. $\ell = 0$) are readily obtained from (3), setting $x = (q, \dot{q}) = (x_p, x_v) \in \mathbb{R}^{2N}$ and $u = m \in \mathbb{R}^N$:

$$(5) \qquad \dot{x} = \begin{bmatrix} x_v \\ -B^{-1}(x_p)n(x) \end{bmatrix} + \begin{bmatrix} O \\ B^{-1}(x_p) \end{bmatrix}u,$$

with $n(q, \dot{q}) = c(q, \dot{q}) + e(q)$ for compactness. Thus, $n = 2N$, $m = N$. As in (1), an output equation can be associated to this dynamic system, typically in the form

$$(6) \qquad y = \begin{cases} q, & \textit{joint space output} \\ k(q), & \textit{cartesian space output} \end{cases}$$

where $p = k(q)$ is the so-called direct kinematics of the arm, a nonlinear mapping $k: \mathbb{R}^N \to \mathbb{R}^N$ in the conventional square case ($p = m = N$). When

the full end-effector pose is considered in vector **p**, a minimal representation should be used for orientation, like Euler or roll-pitch-yaw angles.

In current industrial robots, the nonlinear effects present in the state equations (5) are masked by the adoption of torque transmission elements with a large reduction ratio [3]. However, the demand for accurate end-effector force control, extreme precision in the whole workspace, and high speed in performing automatic tasks, has led to the introduction of a new generation of *direct-drive* arms, i.e. with unitary transmission ratios. For these robots, full consideration of the complex nonlinear and interacting dynamics is unavoidable. Thus, use of standard (approximate) linearization procedures is not adequate, and the motion control problem really asks for nonlinear feedback laws in the form (2). Nonetheless, researchers have soon discovered that, even for direct-drive robots, the general picture is not as bad as it may seem. In fact, in their conventional setting, robot arms *satisfy all* the conditions needed for solving the aforementioned control problems, in particular full linearization and input-output noninteraction. It is easy to see that the suitable feedback and state transformation for the joint output case is

$$(7) \qquad \mathbf{u} = \mathbf{n}(\mathbf{x}) + \mathbf{B}(\mathbf{x}_p)\mathbf{v}, \qquad \Psi(\mathbf{x}) = \mathbf{x},$$

while for the cartesian output is

$$(8) \quad \mathbf{u} = \mathbf{n}(\mathbf{x}) + \mathbf{B}(\mathbf{x}_p)\mathbf{J}^{-1}(\mathbf{x}_p)[-\dot{\mathbf{J}}(\mathbf{x})\mathbf{x}_v + \mathbf{v}], \qquad \Psi(\mathbf{x}) = \begin{bmatrix} \mathbf{k}(\mathbf{x}_p) \\ \mathbf{J}(\mathbf{x}_p)\mathbf{x}_v \end{bmatrix},$$

where $\mathbf{J}(\mathbf{q}) = \partial\mathbf{k}/\partial\mathbf{q}$ is the (square) Jacobian of the direct kinematics. These control laws achieve state and output linearization, in the proper coordinates, and input-output decoupling at the same time, as can be checked by direct inspection. Such a striking result has been labeled in many different ways in robotics, namely as *computed torque*, *inverse dynamics* approach, *resolved-acceleration* method, or *operational space* control. In the cartesian space, slight variations may be encountered depending on the chosen representation of end-effector orientation, but — apart from different algorithmic singularities in the induced Jacobian **J** — a basically unique approach can be resumed [4,5].

In this paper, our purpose is to show that there is more than just 'computed torque' in advanced robotic control problems. There are still plenty of situations needing for an useful transfer of new results from nonlinear control theory. Recently, the notion of *zero dynamics* of a system, i.e. the internal dynamics consistent with the constraint that the system output is zero for all times, has been stated in a precise way also in the nonlinear case [6], providing a convenient tool for the analysis of several control problems and for the generation of powerful results. To mention a few, it has been shown in [7] that invertible systems with no zero dynamics can always be fully linearized by means of *dynamic* state-feedback.

Exponentially stable zero dynamics allows exact or, at least, asymptotic reproduction of output trajectories [8]. In this case, the system is usually referred to as being *minimum phase*. Finally, in the regulation problem for nonlinear systems, solvability conditions can be restated in terms of zero dynamics of the system [9].

In the following, the role of zero dynamics will be investigated with reference to three relevant problems in robotics: control of robots in rigid contact with the environment, free motion control of manipulators with redundant degrees of freedom, and trajectory control of robot arms with flexible links. Increasing interest is being devoted to these robotic applications, which are indeed more complex than conventional ones, but much work has still to be done for obtaining control schemes which perform in a very satisfactory way. Our contribution here is to indicate how the notion of zero dynamics can be used for reinterpreting known results, for providing alternate solutions to challenging problems, or in the definition of new control strategies. Although most of the arguments are presented through examples, we will try to put each case study in the wider perspective of the pertinent robotic field. For completeness, general concepts related to zero dynamics and a computational algorithm are recalled first.

2. Zero dynamics of nonlinear systems

Consider the class of nonlinear systems that are not fully linearizable by feedback. For these systems, the feasibility of a number of control laws is strictly related to the stability properties of a particular dynamics which depends upon the specific control problem faced. When seeking for exact reproduction of output trajectories by means of system inversion, the minimal inverse dynamics is of concern. For input-output noninteracting problems (as well as for disturbance decoupling), the critical issue stands in the dynamics of maximal dimension which can be rendered unobservable via feedback. On the other hand, for solving local stabilization problems using smooth static state-feedback, one should investigate the properties of the internal dynamics when the output is forced to zero. For linear and for nonlinear single-input single-output invertible systems, it is known that the dynamics of the minimal inverse, the dynamics associated with maximal loss of observability under feedback, and the closed-loop dynamics obtained when zeroing the output, are in fact coincident. This equivalence is no longer true for general nonlinear systems [10]. However, these three notions collapse into the same one when the decoupling matrix of the system is nonsingular (or is full row rank, when $p < m$). We shall keep this assumption from now on.

In any case, the stability requirement for the closed-loop system plays the major role in validating any of the previous control designs. Taking advantage of the assumed equivalence of the above three notions, we will focus only on the derivation of the zero dynamics of a given system. Besides,

this is also simpler from a computational point of view, as will be evident in the considered robotic examples.

A coordinate-free algorithm has been given in [8] for computing both the *zero dynamics manifold* $\mathcal{M}^*$, i.e. the set of states that may be assumed by the nonlinear system when the output is constrained to zero, and the *zero dynamics vector field* $f^*(x)|_{\mathcal{M}^*}$, i.e. (the restriction of) a vector field which is always tangent to the manifold $\mathcal{M}^*$. Let x_e be a regular point in the sense of [8], and assume $f(x_e) = 0$ and $h(x_e) = 0$. Denoting by $T_x(M)$ the tangent space at x to M, a sequence $\{M_k\}$ of manifolds can be computed as:

step 0: $M_0 = h^{-1}(0)$;

step k: in a neighborhood $U_{k-1}(x_e)$ such that $U_{k-1} \cap M_{k-1}$ is smooth,

$$M_k = \{x \in U_{k-1} \cap M_{k-1} : f(x) \in \text{span}\,\{g(x)\} + T_x(U_{k-1} \cap M_{k-1})\}.$$

At a step $k^* < n$, this algorithm converges to $\mathcal{M}^* := M_{k^*}$. Moreover, there exists a smooth state-feedback $u = u^*(x)$ such that $f^*(x) := f(x) + g(x)u^*(x)$ is tangent to $\mathcal{M}^*$, and

$$(9) \qquad \dot{x}^* = f^*(x^*), \text{ with } x^* \in \mathcal{M}^* \quad \Rightarrow \quad y = h(x^*(t)) \equiv 0.$$

Since the vector field $f^*(x)$ is tangent to $\mathcal{M}^*$, the restriction $f^*(x)|_{\mathcal{M}^*}$ is a well-defined vector field on $\mathcal{M}^*$. Note that, in local coordinates, the zero dynamics algorithm is similar to the so-called structure algorithm [11]. Moreover, it can be generalized to time-varying constrained outputs and to non-square $(p < m)$ systems, in which case u^* is not unique.

3. Robots in constrained motion

In many industrial tasks, the robot end-effector is required to move in contact with an environmental surface. In such situations, one is interested in controlling motion along selected directions and exchanged forces in some orthogonal ones, thus leading to an *hybrid* control scheme. The task is usually denoted as *compliant*, when some elasticity is assumed at the contact point. This compliant dynamics is due to the non-ideal rigidity of environment and robot, and to the natural deformation of the force/torque sensing device, when present. Experimental evidence shows that the most critical cases arise when the contact stiffness is very high, with the occurrence of an unstable chattering behavior. This motivates the investigation of the limit case, when the contact is perfectly rigid and the end-effector is actually constrained to a given hypersurface.

A general ℓ-dimensional holonomic constraint [2] will be denoted as $\Phi(p) = 0$, being p the end-effector generalized coordinates. Using the arm direct kinematics, this constraint can be rewritten as

$$(10) \qquad \Phi(p) = \Phi(k(q)) = 0, \qquad \Phi : \mathbb{R}^N \to \mathbb{R}^\ell, \; \ell < N.$$

For the constrained robotic system, the right hand side of the overall dynamics (3) becomes, by the principle of virtual work,

$$(11) \qquad m = u + J^T(q)\left(\frac{\partial\Phi}{\partial p}\right)^T F, \qquad u \in \mathbb{R}^N, \; F \in \mathbb{R}^\ell.$$

In (11), u is the control input at the joints $(m = N)$, while F is the generalized constraint force arising at the end-effector. Only compatible forces are generated within this formulation, and these can be interpreted as Lagrange multipliers associated to the given constraint [12]. If simple contact is desired, i.e. with no reaction forces arising at the contact point, vector F plays the role of a disturbance for the system. Accordingly, setting again $x = (q, \dot{q})$, $n = 2N$, and with the ℓ-dimensional vector $z = F$, the state equations assume exactly the form (1). In a similar way, when a contact force $F_d \neq 0$ is desired, the disturbance becomes $z = F - F_d$.

Starting from equation (3) with (11), the following questions will be addressed:

- how do we compute input torques u for staying on the surface $\Phi = 0$?
- how do we express the dynamic behavior on $\Phi = 0$?

A direct answer is provided through the derivation of the zero dynamics of this robotic system, by taking as output to be constrained to zero

$$(12) \qquad y = h(q) = \Phi(k(q)),$$

thus having $p = \ell$ in (1). From

$$(13) \qquad \dot{y} = \frac{\partial h}{\partial q}\dot{q} = T(q)\dot{q}, \qquad \ddot{y} = T(q)\ddot{q} + \dot{T}(q,\dot{q})\dot{q},$$

using the robot dynamic model (3), it is found that $\ddot{y}$ explicitly depends on the input u in a nonsingular way, provided that the $\ell \times N$ *constrained Jacobian* $T = (\partial\Phi/\partial p)J$ is of full rank ℓ. Note that matrix $\dot{T}$ in (13) contains information about the constraint curvature. The zero dynamics manifold $\mathcal{M}^*$ is obtained by setting $y = \dot{y} = 0$:

$$(14) \qquad \mathcal{M}^* = \left\{(q,\dot{q}) \in \mathbb{R}^{2N} : \begin{bmatrix} h(q) \\ T(q)\dot{q} \end{bmatrix} = 0\right\}.$$

From $\ddot{y} = 0$, the state-feedback law which keeps the dynamic flow of the closed-loop system tangent to $\mathcal{M}^*$ is

$$(15)$$
$$u^* = n(q,\dot{q}) - B(q)T^\dagger(q)\dot{T}(q,\dot{q})\dot{q} + B(q)[I - T^\dagger(q)T(q)]v - T^T(q)F,$$
$$= \alpha(x) + \beta(x)v + \gamma(x)z,$$

where $T^\dagger = T^T(TT^T)^{-1}$ is the pseudoinverse of T. This static state-feedback law contains also a disturbance measurement term, i.e. a feedback

from the force sensing device. Also, the new control input $\mathbf{v}$ is premultiplied by the projection matrix into the null space of $\mathbf{T}$. Applying (15), the closed-loop dynamics becomes

$$(16) \qquad \ddot{\mathbf{q}} = -\mathbf{T}^\dagger(\mathbf{q})\dot{\mathbf{T}}(\mathbf{q}, \dot{\mathbf{q}})\dot{\mathbf{q}} + [\mathbf{I} - \mathbf{T}^\dagger(\mathbf{q})\mathbf{T}(\mathbf{q})]\mathbf{v},$$

which is a set of N second-order differential equations. Since the projection matrix has rank $N - \ell$, this will also be the actual number of *independent* control inputs, out of the N components of $\mathbf{v}$. When the initial conditions are specified on $\mathcal{M}^*$, all solutions of (16) will 'live' in the lower dimensional manifold $\mathcal{M}^*$ onto which the dynamical system is projected.

To display correctly the zero dynamics, the vector field $\mathbf{f}^*$, implicitly defined within (16), has to be restricted to $\mathcal{M}^*$. Thus, instead of project-ing, we should *reduce* equations. In order to do so, a proper change of coordinates is needed:

$$(17) \qquad \xi = \begin{bmatrix} \xi_1 \\ \xi_2 \\ \xi_3 \\ \xi_4 \end{bmatrix} = \begin{bmatrix} \mathbf{h}(\mathbf{q}) \\ \mathbf{T}(\mathbf{q})\dot{\mathbf{q}} \\ \mathbf{q}_r \\ \dot{\mathbf{q}}_r \end{bmatrix},$$

where $\mathbf{q}_r \in I\!\!R^{N-\ell}$ (a subpart of $\mathbf{q}$) is used as a local parametrization of the constraint surface. Then, the reduced set of $2(N - \ell)$ first-order equations expressing the zero dynamics of the robot system in constrained motion is

$$(18) \qquad \dot{\xi}_3 = \xi_4, \qquad \dot{\xi}_4 = \Gamma(0, 0, \xi_3, \xi_4, \mathbf{a}),$$

being $\mathbf{a}$ the reduction to $\mathcal{M}^*$ of the forcing term $\mathbf{v}$ in (16). This dynamics describes in terms of joint coordinates the motion of the robot end-effector on the surface $\Phi = 0$. Input $\mathbf{a}$ can be used to stabilize this motion, indepen-dently of the constraint forces acting in the span of the rows of $(\partial\Phi/\partial\mathbf{p})^T$. This interpretation is in the same spirit of hybrid control schemes [13], in which dynamic decoupling of force and velocity control loops can be obtained via a nonlinear feedback similar to (15). Also, the proposed ap-proach is consistent with the results derived in [12]. An example will further illustrate the above concepts.

Example. Consider a planar RP (cylindric) robot arm, moving the end-effector in rigid contact with a circular surface of radius r, as in Fig. 1. In this case, $N = 2$, $\ell = 1$, and

$$(19) \qquad \phi(\mathbf{p}) = p_x^2 + p_y^2 - r^2 = 0, \quad \text{or} \quad h(\mathbf{q}) = q_2 - r = 0,$$

showing that the end-effector constraint maps into a linear one in the joint space. The dynamic model of this robot arm is

$$(20)$$
$$\begin{bmatrix} b_{11}(q_2) & 0 \\ 0 & b_{22} \end{bmatrix}\begin{bmatrix} \ddot{q}_1 \\ \ddot{q}_2 \end{bmatrix} + \begin{bmatrix} n_1(q_2, q_1, \dot{q}_2) \\ n_2(q_2, \dot{q}_1) \end{bmatrix} = \begin{bmatrix} u_1 \\ u_2 \end{bmatrix} + \begin{bmatrix} -q_2 s_1 & q_2 c_1 \\ c_1 & s_1 \end{bmatrix}\begin{bmatrix} 2p_x \\ 2p_y \end{bmatrix}F,$$

with the usual notation $s_i = \sin q_i$, $c_i = \cos q_i$. The scalar value F, the force acting in the direction normal to the constraint surface, is directly available from a sensor measurement.
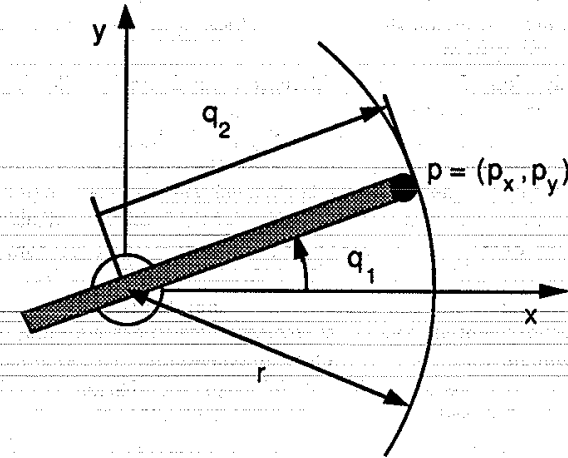

Fig. 1 – A planar RP robot in constrained motion

Simplifications are introduced when the constraint is expressed in joint coordinates, since

$$(21) \quad \mathbf{T}(\mathbf{q}) = \frac{\partial h(\mathbf{q})}{\partial \mathbf{q}} = [0 \quad 1], \quad \dot{\mathbf{T}} = 0, \quad \mathbf{T}^\dagger = \begin{bmatrix} 0 \\ 1 \end{bmatrix}, \quad \mathbf{I} - \mathbf{T}^\dagger\mathbf{T} = \begin{bmatrix} 1 & 0 \\ 0 & 0 \end{bmatrix}.$$

Then, the nonlinear feedback control (15) takes the form

$$(22) \qquad \mathbf{u}^* = \begin{bmatrix} n_1(q_2, \dot{q}_1, \dot{q}_2) + b_{11}(q_2)v_1 \\ n_2(q_2, \dot{q}_1) - F \end{bmatrix},$$

assuming that the desired contact force is zero. This control law becomes a linear one when evaluated on $\mathcal{M}^* = \{(\mathbf{q}, \dot{\mathbf{q}}) \in I\!\!R^4 : q_2 - r = 0, \dot{q}_2 = 0\}$, with $u_1^* = b_{11}(r)v_1$, $u_2^* = -F$. The closed-loop dynamics (16) collapses into $\ddot{\mathbf{q}} = [v_1 \ 0]^T$ so that, selecting $\mathbf{q}_r = q_1$ and $\mathbf{a} = v_1$, the zero dynamics reduces simply to $\ddot{q}_1 = v_1$. Note that in this case q_1 parametrizes *globally* the constraint surface. ∎

4. Redundant robot arms

Kinematic redundancy in robot arms is a relative concept. A robot is said to be redundant when the number N of degrees of freedom (viz. of joints) is larger than p, the number of coordinates strictly needed for describing a

given compatible task. For instance, a planar 3-dof arm is redundant for the end-effector *positioning* task, but it is not if also the *orientation* around an axis normal to the plane is of concern. The 'primary' task is often specified in terms of the robot end-effector variables, as in this example. Therefore, it is convenient to define these task variables as characterizing outputs for the redundant system.

Introduction of redundancy increases arm dexterity, allowing collision avoidance with workspace obstacles or enabling to comply with joint range limits. Most important, it provides the manipulator with the capability of avoiding singular configurations, where the kinematics Jacobian looses full rank. A nice analytic feature is that one can associate significant performance indices to all these problems, e.g. the minimum distance of the arm from an obstacle. The robot additional degrees of freedom can then be used for optimizing these performance criteria during local or global motion. Similarly, one can exploit redundancy for the satisfaction of secondary or 'augmented' tasks. A review of the most common resolution schemes can be found in [14]. On the other hand, the kinematic transformation of end-effector paths into joint-space paths for redundant arms is not straightforward, due to the non-existence of a closed-form solution or, equivalently, to the presence of an infinite number of admissible inverse solutions. This complexity is inherited also at the dynamic and control levels. The fact that different arm postures may correspond to the same end-effector location induces some specific undesirable issues that can be classified as follows:

- *non-repeatability:* a cyclic behavior of the task variables may not correspond to a cyclic behavior of the joint variables;
- *self-motions:* a non-zero joint velocity may still be present though the end-effector is fixed at a given point, even for nonsingular arm configurations.

These two problems depend on the particular resolution strategy that is being used. If redundancy is controlled at a kinematic level using a *homogeneous* law of the form $\dot{\mathbf{q}} = \mathbf{H}(\mathbf{q})\dot{\mathbf{p}}$, necessary and sufficient conditions for obtaining a repeatable motion have been stated in [15], requiring the involutivity of the columns of $\mathbf{H}$. Note that a repeatable behavior can be considered as a stability property in the large.

Here, we will be mainly interested in the control of self-motions. In particular, we would like to design a control law which stabilizes the internal arm configuration around a desired equilibrium, while keeping the end-effector at the fixed location $\bar{\mathbf{p}}$. The notion of zero dynamics is again helpful in finding a solution to this problem. For, define as output

(23) $\mathbf{y} = \mathbf{h}(\mathbf{q}) = \mathbf{k}(\mathbf{q}) - \bar{\mathbf{p}},$ with $\bar{\mathbf{p}}$ fixed,

and since

(24) $\dot{\mathbf{y}} = \mathbf{J}(\mathbf{q})\dot{\mathbf{q}},$ $\ddot{\mathbf{y}} = \mathbf{J}(\mathbf{q})\ddot{\mathbf{q}} + \dot{\mathbf{J}}(\mathbf{q},\dot{\mathbf{q}})\dot{\mathbf{q}},$

an explicit dependence of $\ddot{\mathbf{y}}$ on $\mathbf{u}$ is found through the dynamic model $\mathbf{B}(\mathbf{q})\ddot{\mathbf{q}} + \mathbf{n}(\mathbf{q},\dot{\mathbf{q}}) = \mathbf{u}$. Setting $\mathbf{y} = \dot{\mathbf{y}} = 0$, the zero dynamics manifold follows as

$$(25) \qquad \mathcal{M}^* = \left\{ (\mathbf{q},\dot{\mathbf{q}}) \in I\!\!R^{2N} : \begin{bmatrix} \mathbf{k}(\mathbf{q}) - \bar{\mathbf{p}} \\ \mathbf{J}(\mathbf{q})\dot{\mathbf{q}} \end{bmatrix} = 0 \right\}.$$

From $\ddot{\mathbf{y}} = 0$, all control inputs making $\mathcal{M}^*$ invariant have the form

$$(26) \qquad \mathbf{u}^* = \mathbf{n}(\mathbf{q},\dot{\mathbf{q}}) - \mathbf{B}(\mathbf{q})\mathbf{J}^\dagger(\mathbf{q})\dot{\mathbf{J}}(\mathbf{q},\dot{\mathbf{q}})\dot{\mathbf{q}} + \mathbf{B}(\mathbf{q})[\mathbf{I} - \mathbf{J}^\dagger(\mathbf{q})\mathbf{J}(\mathbf{q})]\mathbf{v},$$

which yields in the closed loop

$$(27) \qquad \ddot{\mathbf{q}} = -\mathbf{J}^\dagger(\mathbf{q})\dot{\mathbf{J}}(\mathbf{q},\dot{\mathbf{q}})\dot{\mathbf{q}} + [\mathbf{I} - \mathbf{J}^\dagger(\mathbf{q})\mathbf{J}(\mathbf{q})]\mathbf{v},$$

where the second term on the right hand side is a joint acceleration vector lying in the null space of the Jacobian $\mathbf{J}$. Note that the closed-loop system is described by purely kinematic equations, because dynamic terms have already been cancelled via feedback. Although equation (27) — just as (16) — does not describe correctly the zero dynamics of the redundant system, yet it is a suitable basis for the design of an external input $\mathbf{v}$ which stabilizes the arm around the desired equilibrium configuration $(\mathbf{q},\dot{\mathbf{q}}) = (\mathbf{q}_d, 0)$. Since $\mathbf{q}_d$ may not be consistent with the fixed $\bar{\mathbf{p}}$ (i.e. $\mathbf{k}(\mathbf{q}_d) \neq \bar{\mathbf{p}}$), it is reasonable to define a *projected* state error

$$(28) \qquad \mathbf{E} = [\mathbf{I} - \mathbf{J}^\dagger(\mathbf{q})\mathbf{J}(\mathbf{q})][\mathbf{K}_P(\mathbf{q}_d - \mathbf{q}) - \dot{\mathbf{q}}], \qquad \mathbf{K}_P > O,$$

in which any suitable gain scaling matrix may be chosen for $\mathbf{K}_P$, e.g. the identity. This error term will be zeroed using the following result, which provides thus a stabilizing control law for self-motions of redundant arms.

Theorem. *For the dynamics (27), the choice*

$$(29) \qquad \mathbf{v} = -\mathbf{K}_P\dot{\mathbf{q}} + \mathbf{K}_E\mathbf{E} - \mathbf{J}^\dagger\mathbf{J}[\mathbf{K}_P(\mathbf{q}_d - \mathbf{q}) - \dot{\mathbf{q}}],$$

with $\mathbf{K}_E > O$, is such that the projected error $\mathbf{E}$ in (28) asymptotically tends to zero.

Proof. Define a Lyapunov candidate as $V = \frac{1}{2}\mathbf{E}^T\mathbf{E}$, and note that

$$(30) \qquad \dot{\mathbf{E}} = -[\mathbf{I} - \mathbf{J}^\dagger\mathbf{J}](\mathbf{v} + \mathbf{K}_P\dot{\mathbf{q}}) - [\dot{\mathbf{J}}^\dagger\mathbf{J} + \mathbf{J}^\dagger\dot{\mathbf{J}}][\mathbf{K}_P(\mathbf{q}_d - \mathbf{q}) - \dot{\mathbf{q}}],$$

and

$$(31) \qquad \mathbf{E}^T[\dot{\mathbf{J}}^\dagger\mathbf{J} + \mathbf{J}^\dagger\dot{\mathbf{J}}] = \mathbf{E}^T\mathbf{J}^\dagger\dot{\mathbf{J}}.$$

Since the projection matrix is idempotent, using $\mathbf{E}^T[\mathbf{I} - \mathbf{J}^\dagger \mathbf{J}] = \mathbf{E}^T$, and applying (29) gives

$$(32) \quad \begin{aligned} \dot{V} = \mathbf{E}^T \dot{\mathbf{E}} &= -\mathbf{E}^T(\mathbf{v} + \mathbf{K}_P \dot{\mathbf{q}}) - \mathbf{E}^T[\dot{\mathbf{J}}^\dagger \mathbf{J} + \mathbf{J}^\dagger \dot{\mathbf{J}}][\mathbf{K}_P(\mathbf{q}_d - \mathbf{q}) - \dot{\mathbf{q}}] \\ &= -\mathbf{E}^T \mathbf{K}_E \mathbf{E} \le 0. \end{aligned}$$

Note that the assumption of full row rank for $\mathbf{J}$ is never needed, contrary to the arguments used in [16].   Q.E.D.

The obtained stabilization is performed according to projection rules. However, if the zero dynamics concept is exploited in full, one can show that stabilization may be achieved working only within the reduced zero dynamics submanifold. This will be illustrated in the following example.

Example. Consider a planar PPR-robot arm ($N = 3$) with the third link of length ℓ (see Fig. 2). For the task of positioning the end-effector

$$(33) \quad p_x = q_1 + \ell c_3, \quad p_y = q_2 + \ell s_3,$$
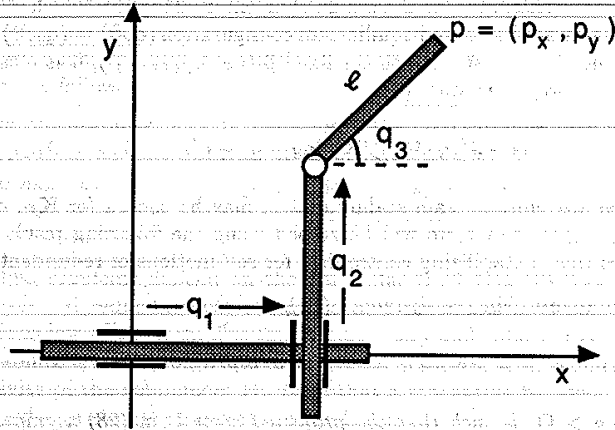
this robot is redundant.

Fig. 2 – A planar PPR robot arm

The Jacobian matrix

$$(34) \quad \mathbf{J} = \begin{bmatrix} 1 & 0 & -\ell s_3 \\ 0 & 1 & \ell c_3 \end{bmatrix}$$

is always of full rank, and so its pseudoinverse $\mathbf{J}^\dagger$ and the projection matrix

in the null space of $\mathbf{J}$ have the explicit expressions

$$(35) \quad \mathbf{J}^\dagger = \frac{1}{1+\ell^2} \begin{bmatrix} 1 + \ell^2 c_3^2 & \ell^2 s_3 c_3 \\ \ell^2 s_3 c_3 & 1 + \ell^2 s_3^2 \\ -\ell s_3 & \ell c_3 \end{bmatrix},$$

$$\mathbf{I} - \mathbf{J}^\dagger \mathbf{J} = \frac{1}{1+\ell^2} \begin{bmatrix} \ell s_3 \\ -\ell c_3 \\ 1 \end{bmatrix} \begin{bmatrix} \ell s_3 & -\ell c_3 & 1 \end{bmatrix}.$$

We first show that, taking $\mathbf{v} = 0$ instead of (29) in (27), an undesirable limit cycle may be induced as a self-motion of the arm. In fact, the closed-loop dynamics becomes in this case

$$(36) \quad \ddot{\mathbf{q}} = -\mathbf{J}^\dagger \dot{\mathbf{J}} \dot{\mathbf{q}} = \begin{bmatrix} \ell \dot{q}_3^2 c_3 \\ \ell \dot{q}_3^2 s_3 \\ 0 \end{bmatrix},$$

so that, entering at $t = t_0$ a fixed location $\mathbf{p} = \bar{\mathbf{p}} = (\bar{p}_x, \bar{p}_y)$, with $\dot{\mathbf{p}} = 0$, and having, say, $q_3(t_0) = 0$ but $\dot{q}_3(t_0) = \gamma \ne 0$, would give

$$(37) \quad \begin{aligned} q_1(t) &= \bar{p}_x - \ell \cos \gamma(t - t_0), \\ q_2(t) &= \bar{p}_y - \ell \sin \gamma(t - t_0), \\ q_3(t) &= \gamma(t - t_0), \end{aligned}$$

i.e. an endless harmonic motion of the two prismatic joints. On the other hand, there is a stabilizing strategy to be pursued which is also more direct than (29). The idea is to reparametrize the robot joint coordinates in terms of q_3 and $\dot{q}_3$ only

$$(38) \quad \begin{aligned} q_1 &= \bar{p}_x - \ell c_3 = g_1(q_3), & q_2 &= \bar{p}_y - \ell s_3 = g_2(q_3), \\ \dot{q}_1 &= \ell \dot{q}_3 s_3 = g_3(q_3, \dot{q}_3), & \dot{q}_2 &= -\ell \dot{q}_3 c_3 = g_4(q_3, \dot{q}_3), \end{aligned}$$

so that the zero dynamics manifold can be characterized as

$$(39) \quad \mathcal{M}^* = \{(\mathbf{q}, \dot{\mathbf{q}}) \in I\!R^6 : q_1 = g_1(q_3), \; q_2 = g_2(q_3), \; \dot{q}_1 = g_3(q_3, \dot{q}_3), \; \dot{q}_2 = g_4(q_3, \dot{q}_3)\}$$

while the zero dynamics is just $\ddot{q}_3 = v_3$. This will be *globally* stabilized at the value q_{d3} by choosing $v_3 = K_p(q_{d3} - q_3) - K_v \dot{q}_3$, with K_p, K_v both positive. Although kinematically simple, this robot is not a trivial case. For instance, it is interesting to remark that solving redundancy by pseudoinversion, i.e. choosing $\dot{\mathbf{q}} = \mathbf{J}^\dagger(\mathbf{q})\dot{\mathbf{p}}$, does not yield a repeatable solution. The necessary and sufficient condition is that the columns $\mathbf{j}_i^\dagger$ of $\mathbf{J}^\dagger$, seen as vector fields, are involutive. However, this is not the case since

$$(40) \quad [\mathbf{j}_1^\dagger, \mathbf{j}_2^\dagger] \propto \begin{bmatrix} \ell s_3 \\ -c_3 \\ 1 \end{bmatrix} \notin \text{span}\{\mathbf{j}_1^\dagger, \mathbf{j}_2^\dagger\},$$

where $[j_1^l, j_2^l] = (\partial j_2^l/\partial q)j_1^l - (\partial j_1^l/\partial q)j_2^l$ is the Lie bracket of the two vector fields [1]. ∎

The proposed stabilizing strategy for self-motions could be generalized to the case $\dot{p} \neq 0$, and used for keeping under control the robot joint velocity. We conclude this section by noting that the idea of reparametrization of redundant robots and of *reduction* to a lower-dimensional manifold has been explored also for optimization purposes in [17,18].

5. Robots with flexible elements

There are two types of possible deformation in robots, namely joint elasticity and link flexibility. Joint elasticity is introduced by transmission elements like harmonic drives, belts, or long shafts, and is the basic source of vibration in industrial arms with massive links [19]. The dynamic model of robots with elastic joints is obtained by doubling the number of generalized coordinates, using one variable for the actuator position and a different one for the link position. The resulting model is described by $2N$ second order differential equations of the form (3), but with only half of the components of m available for control (i.e. $m = [I_{N \times N} \; O_{N \times N}]^T u$, up to a row permutation). Link flexibility, instead, is non negligible for long and/or lightweight arms, like the Space Shuttle Remote Manipulator. Although deflection is distributed in nature, finite-dimensional dynamic models are usually derived, by representing each link as an Euler beam with proper boundary conditions and limiting to N_e the number of modal functions in the associated small deformation eigenvalue problem. Alternatively, the methods of finite elements or of assumed modes can be used for directly approximating the link deflection [20]. Using the Lagrangian approach, the coupling of N rigid motion equations with N_e flexible ones will result in a nonlinear dynamic model that is still in the form (3), but now with $m = [I_{N \times N} \; O_{N \times N_e}]^T u$.

Various motion control objectives can be pursued in the presence of flexibility, ranging from point-to-point control with vibrational damping to accurate trajectory tracking. Indeed, trajectories specified at the actuator level produce a different and oscillatory behavior at the end-effector level, both for the elastic joint and for the flexible link case. In spite of this analogy, the trajectory tracking control problem is completely different in the two cases. The basic issue is summarized in the following question:

- is it possible for robots with flexible elements to find an input torque so to exactly reproduce a desired (smooth) end-effector trajectory?

This can be restated as finding whether the computed torque method can be extended also to flexible robot arms. The answer is always positive for robots with joint elasticity. When controlling the end-effector or the link position — both outputs being *beyond* the elasticity — of these robots, one is dealing with an invertible nonlinear system having *no zero dynamics*.

Therefore, by the use of static [21] or, when needed, dynamic [22] inversion-based state-feedback, a fully linear closed-loop system can be obtained, equivalent to a set of independent strings of input-output integrators of length greater than or equal to four. These results closely mimic the ones obtained for conventional rigid robots.

In the case of link flexibility, the trajectory tracking problem is much more involved. Instead of following a general but cumbersome formalism, we will focus on a one-link planar flexible arm, modeling just one deflection mode ($N_e = 1$). This finite-dimensional model, although of reduced-order, is still a representative one in the sense that it displays the same basic control properties of more accurate and/or distributed models. It will be shown that the zero dynamics is useful in the study of the tracking problem, and it is crucial in the design of outputs for which exact trajectory reproduction can be achieved in a stable fashion via inversion control. In particular, the zero-dynamics analysis will provide a constructive answer to the question of finding the input that produces a desired end-effector trajectory.

Example. Consider the one-link flexible arm of Fig. 3, moving on the horizontal plane. Following the general modeling technique proposed in [23], based on the Ritz-Kantorovitch expansion for approximating link deformation, we assume here second-degree polynomials as basis functions. Imposing geometric boundary conditions of the 'clamped' type at the link base, it turns out that a parabolic shape is sufficient to describe the pure bending deformation of the link.
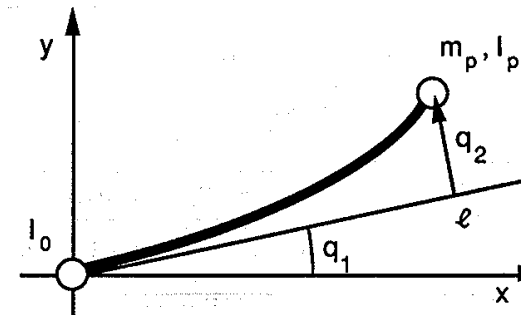

Fig. 3 – A one-link flexible robot arm

Let ℓ be the length of the uniform link and m its mass, I_o the inertia of the hub, m_p and I_p the mass and inertia of a payload located at the tip, and u the input torque. The angular position q_1 of the link base and the deflection q_2 at the tip point are chosen as generalized coordinates. If the analysis is not limited to small deflections, a nonlinear dynamic model is

obtained in the standard form

$$(41) \quad \begin{bmatrix} b_{11}(q_2) & b_{12} \\ b_{12} & b_{22} \end{bmatrix} \begin{bmatrix} \ddot{q}_1 \\ \ddot{q}_2 \end{bmatrix} + \begin{bmatrix} c_1(q_2, \dot{q}_1, \dot{q}_2) \\ c_2(q_2, \dot{q}_1) + kq_2 \end{bmatrix} = \begin{bmatrix} 1 \\ 0 \end{bmatrix} u,$$

with elements of the inertia matrix $\mathbf{B}(q_2)$ and Coriolis and centrifugal terms given by

$$(42) \quad b_{11}(q_2) = a + bq_2^2, \qquad b_{12} = c, \qquad b_{22} = d,$$
$$c_1(q_2, \dot{q}_1, \dot{q}_2) = 2bq_2\dot{q}_1\dot{q}_2, \quad c_2(q_2, \dot{q}_1) = -bq_2\dot{q}_1^2,$$

where

$$(43) \quad a = I_o + \frac{1}{3}m\ell^2 + I_p + m_p\ell^2, \quad b = \frac{1}{5}m + m_p,$$
$$c = \frac{1}{4}m\ell + \frac{2}{\ell}I_p + m_p\ell, \quad d = \frac{1}{5}m + \frac{4}{\ell^2}I_p + m_p.$$

In (41), $k = 4EI/\ell^3$ is the link elasticity coefficient, with Young modulus E and link cross sectional inertia I. State equations are derived by setting $\mathbf{x} = (q_1, q_2, \dot{q}_1, \dot{q}_2) \in I\!R^4$. For trajectory control, a scalar output can be conveniently defined as the angular position of a generic point along the link, as seen from the base. For simplicity, a linearized version of this output will be used. Its parametric expression is

$$(44) \quad y(\lambda) = q_1 + \frac{\lambda}{\ell}q_2, \qquad \lambda \in [0,1].$$

For $\lambda = 0$, the output is the joint angle, while for $\lambda = 1$, the output is the angular position of the tip. Being interested in tracking end-effector trajectories, one should consider mainly $y(1)$. Unfortunately, with this choice inversion control, which is the strategy used to guarantee exact tracking, leads in general to an unstable closed-loop behavior. This is because of the presence of an *unstable zero dynamics* that limits the application of pure inversion control, and is consistent with the usual non-minimum phase characteristics of the transfer function from joint torque to tip position in linear dynamic models of one-link flexible arms [24]. However, the actual situation is more tricky and it is interesting to see for what values of λ, i.e. for which output, it is still possible to reproduce exactly a trajectory. For this purpose, an explicit expression should be derived for the system zero dynamics. The relative degree of output (44) is two, except for a particular parameter value λ_0 which will be characterized later. Then, the synthesis of an inversion-based control is accomplished deriving twice the output, setting $\ddot{y} = v$, and solving for u:

$$(45) \quad u = c_1(q_2, \dot{q}_1, \dot{q}_2) - \frac{b_{12} - \frac{\lambda}{\ell}b_{11}(q_2)}{b_{22} - \frac{\lambda}{\ell}b_{12}}(c_2(q_2, \dot{q}_1) + kq_2)$$
$$+ \frac{\det \mathbf{B}(q_2)}{b_{22} - \frac{\lambda}{\ell}b_{12}}v = \alpha(\mathbf{x}) + \beta(\mathbf{x})v.$$

Using the linear change of coordinates $\tilde{\mathbf{x}} = \Psi(\mathbf{x}) = (y, \dot{y}, q_2, \dot{q}_2)$, the closed-loop equations become

$$\ddot{y} = v,$$
$$(46) \quad \ddot{q}_2 = \frac{c_2(\dot{y}, q_2, \dot{q}_2) + kq_2}{\frac{\lambda}{\ell}b_{12} - b_{22}} + \frac{b_{12}}{\frac{\lambda}{\ell}b_{12} - b_{22}}v.$$

It is easy to see that the zero dynamics, restricted to the manifold $\mathcal{M}^* = \{(\mathbf{q}, \dot{\mathbf{q}}) \in I\!R^4 : q_1 = -\frac{\lambda}{\ell}q_2, \dot{q}_1 = -\frac{\lambda}{\ell}\dot{q}_2\}$, represents in this case the dynamics of the flexible variable q_2, evaluated for $y(t) \equiv 0$:

$$(47) \quad \ddot{q}_2 = \frac{[k - b(\frac{\lambda}{\ell})^2\dot{q}_2^2]q_2}{\frac{\lambda}{\ell}c - d} = \frac{[k - b(\frac{\lambda}{\ell})^2\dot{q}_2^2]q_2}{\Delta(\lambda)}.$$

The stability properties of this two-dimensional dynamics can be studied for different values of λ. Whenever the zero dynamics will be found to be asymptotically stable, the following choice for v

$$(48) \quad v = \ddot{y}_d + K_D(\dot{y}_d - \dot{y}) + K_P(y_d - y), \qquad K_P, K_D > 0,$$

will guarantee asymptotic tracking of $y_d(t)$, or even exact tracking for matched initial conditions. In particular, for $\lambda = 0$, the linear zero dynamics $\ddot{q}_2 = -(k/d)q_2$ is found, having two complex poles on the imaginary axis. The presence of some structural damping in the model would force exponential stability. It follows immediately that joint trajectories can be always tracked in a stable fashion. This is a general conclusion for robots with flexible links, holding even in the multi-link, multi-modal case. For $\lambda > 0$, it can be assumed that the (state-dependent) coefficient of q_2 in the numerator of (47) remains positive, as it is when testing stability in the first approximation. Therefore, the properties of the zero dynamics will depend only on the sign of the denominator Δ, a function of the parameter λ. The stability condition can be rewritten more explicitly as

$$(49) \quad \Delta(\lambda) = (\frac{\lambda}{4} - \frac{1}{5})m + (\lambda - 1)m_p + (2\lambda - 4)\frac{I_p}{\ell^2} < 0.$$

In the absence of a payload ($m_p = I_p = 0$), asymptotic stability is obtained for all $\lambda \in [0, 4/5)$. Then, the inversion controller (45), with (48), will 'stiffen' the behavior of any output point which is up to four fifth of the link length ℓ, letting it trace the desired trajectory while keeping the arm deformation bounded. On the other hand, choosing an output associated to $\lambda > 4/5$ will lead to an unbounded state evolution, once inversion control is applied. The transition from stable to unstable behavior occurs at that link point corresponding to $\lambda_0 = 4/5$, where the relative degree is larger than two. This particular point can be physically visualized, in terms of *in phase* or *out of phase* motion. In fact, with the undeformed arm initially

at rest, this point will have zero acceleration at time $t = 0^+$ in response to a step input torque applied at time $t = 0^-$ at the joint, and will separate positive from negative acceleration points. However, note that the location of such a point along the link depends on the mechanical characteristics of the arm. If the robot arm is loaded with a concentrated tip mass $m_p = k_1 m$ ($I_p = 0$), then

$$(50) \qquad \Delta(\lambda) < 0 \iff 0 \le \lambda < \frac{20k_1 + 4}{20k_1 + 5} < 1,$$

and by increasing the payload mass via k_1, the transition point will move closer to the tip, although never reaching it. On the other hand, assuming the payload mass negligible ($m_p \approx 0$) with respect to its inertia $I_p = k_2 m \ell^2$, one has

$$(51) \qquad \Delta < 0 \iff 0 \le \lambda < \frac{80k_2 + 4}{40k_2 + 5},$$

so that the same positive benefit is obtained for a sufficiently large k_2. Moreover, in this case the critical point λ_0 becomes greater than unity for $k_2 > 0.025$. As a consequence, by mechanically increasing tip inertia, *also* an end-effector trajectory can be exactly reproduced in a stable fashion using inversion control. Stated differently, the tip point is not anymore a non-minimum phase output, according to the stability achieved for the associated zero dynamics. ∎

Combining the above two ideal analyses leads to similar results for a real payload, with both non-zero mass and inertia. This formal result is also confirmed by common experience: in fact, it is much easier to control the end-point motion of a flexible arm when this is subject to heavy (relative to the link mass) loading at the tip. The numerical simulations reported in [25] for a slightly different model of the flexible arm, display the effects of different feasible choices for λ. Performance of the resulting controllers are evaluated in terms of tip motion accuracy and control effort. When $\lambda_0 < 1$, increasing λ in the feasible range $[0, \lambda_0)$ produces remarkable improvements in the end-effector trajectory tracking.

A final comment is in order about the occurrence of instability in case of non-minimum phase output. When the zero-dynamics is unstable, inverse control substantially leads to an unbounded state evolution in the closed loop. However, it is possible to show that there exists a particular initial condition for the arm, depending on the desired trajectory, which still guarantees an overall bounded evolution under pure inversion control. Computation of this initial condition is a by-product of the output regulation theory for nonlinear systems [9]. Further analysis and numerical results for a flexible robot can be found in [26]. We just note here that, if the arm is in a different initial state (e.g. typically undeformed), *only* the

regulator approach is capable of achieving asymptotic output tracking with bounded internal state. However, if a non-causal solution is admitted [27], one may also find an input torque to be applied for $t < 0$, i.e. before the start of the actual trajectory, so to lead the system in the required initial condition at time $t = 0$.

6. Conclusions

Robotics proposes several interesting problems where advanced nonlinear control techniques find a natural application. Beside feedback linearization for conventional rigid manipulators or exact linearization via dynamic feedback for robots with joint elasticity, we believe that use of more recently developed nonlinear tools could also lead to similar relevant results. We have shown here that an important role can be recognized for the notion of zero dynamics of a system.

Zero dynamics was investigated here in relation to some special robotic control problems. Robots in constrained maneuvers were revisited in this key, interpreting the zero dynamics as the description of the end-effector motion on the constraining surface. This provides also a basis for understanding the intrinsic decoupling achievable in the hybrid control of normal force and of tangential velocity. The problem of controlling self-motions in redundant arms, treated from the point of view of zero dynamics, led to the statement of a new stabilization result. The given analysis supports the conclusion that, for stabilizing purposes, it is sufficient to work in the reduced space of the extra degree of freedoms. In the trajectory control problem for robot arms with flexible links, the stability condition for the zero dynamics was found to be a clean guide in selecting system outputs to be used for inversion. In particular, a set of alternate control strategies can be generated by re-locating the output point within a feasible range along the link. The chosen approach proved helpful also for showing that the non-minimum phase property of the end-effector control problem strongly depends on the mechanical characteristics of the flexible arm — an aspect which is often overlooked.

We finally remark that the scope of the obtained results is not limited to the relatively simple case studies presented. Ultimately, the unifying perspective offered by the notion of zero dynamics has provided a deeper understanding of the considered robotic control problems.

Acknowledgements

REFERENCES

[1] A. Isidori, *Nonlinear Control Systems*, 2nd Edition, Springer Verlag, Berlin, 1989.

[2] H. Goldstein, *Classical Mechanics*, Addison-Wesley, Reading, 1980.

[3] H. Asada and J.-J.E. Slotine, *Robot Analysis and Control*, John Wiley, New York, 1986.

[4] T.J. Tarn, A.K. Bejczy, A. Isidori, and Y. Chen, "Nonlinear feedback in robot arm control," *Proc. 23rd IEEE Conf. on Decision and Control* (Las Vegas, NV, Dec. 12-14, 1984), pp. 736-751.

[5] K. Kreutz, "On manipulator control by exact linearization," *IEEE Trans. on Automatic Control*, vol. AC-34, no. 7, pp. 763-767, 1989.

[6] C. Byrnes and A. Isidori, "Local stabilization of critically minimum phase nonlinear systems," *Systems and Control Lett.*, vol. 11, no. 1, pp. 9-17, 1988.

[7] A. Isidori, C.H. Moog, and A. De Luca, "A sufficient condition for full linearization via dynamic state feedback," *Proc. 25th IEEE Conf. on Decision and Control* (Athens, GR, Dec. 10-12, 1986), pp. 203-208.

[8] C. Byrnes and A. Isidori, "Asymptotic properties of nonlinear minimum phase systems," in *New Trends in Nonlinear Control Theory*, J. Descusse, M. Fliess, A. Isidori, and D. Leborgne Eds., Lecture Notes in Control and Information Sciences, vol. 122, pp. 254-264, Springer Verlag, 1989.

[9] A. Isidori and C. Byrnes, "Output regulation of nonlinear systems," *IEEE Trans. on Automatic Control*, vol. AC-35, no. 2, pp. 131-140, 1990.

[10] A. Isidori and C.H. Moog, "On the nonlinear equivalent of the notion of transmission zeros," in *Modelling and Adaptive Control*, C.I. Byrnes and A. Kurzhanski Eds., Lecture Notes in Control and Information Sciences, vol. 105, pp. 146-158, Springer Verlag, 1988.

[11] S.N. Singh, "A modified algorithm for invertibility in nonlinear systems," *IEEE Trans. on Automatic Control*, vol. AC-26, no. 2, pp. 595-598, 1981.

[12] N.H. McClamroch and D. Wang, "Feedback stabilization and tracking in constrained robots," *IEEE Trans. on Automatic Control*, vol. AC-33, no. 5, pp. 419-426, 1988.

[13] A. De Luca, C. Manes, and F. Nicolò, "A task space decoupling approach to hybrid control of manipulators," *Proc. 2nd IFAC Symp. on Robot Control (SYROCO'88)* (Karlsruhe, FRG, Oct. 5-7, 1988), pp. 157-162.

[14] D.N. Nenchev, "Redundancy resolution through local optimization: a review," *J. of Robotic Systems*, vol. 6, no. 6, pp. 769-798, 1989.

[15] T. Shamir and Y. Yomdin, "Repeatability of redundant manipulators: mathematical solution of the problem," *IEEE Trans. on Automatic Control*, vol. AC-33, no. 11, pp. 1004-1009, 1988.

[16] P. Hsu, J. Hauser, and S. Sastry, "Dynamic control of redundant ma-

nipulators," *J. of Robotic Systems*, vol. 6, no. 2, pp. 133-148, 1989.

[17] A. De Luca and G. Oriolo, "The reduced gradient method for solving redundancy in robot arms," *Prepr. 11th IFAC World Congress* (Tallinn, Estonia, Aug. 13-17, 1990), vol. 9, pp. 143-148.

[18] A. De Luca and G. Oriolo, "Efficient dynamic resolution of robot redundancy," *Proc. 1990 American Control Conf.* (San Diego, CA, May 23-25, 1990), pp. 221-227.

[19] M.C. Good, L.M. Sweet, and K.L. Strobel, "Dynamic models for control system design of integrated robot and drive systems," *ASME J. of Dynamic Systems, Measurement, and Control*, vol. 107, no. 3, pp. 53-59, 1985.

[20] L. Meirovitch, *Analytical Methods in Vibrations*, Macmillan, New York, 1967.

[21] M.W. Spong, "Modeling and control of elastic joint robots," *ASME J. of Dynamic Systems, Measurement, and Control*, vol. 109, no. 3, pp. 310-319, 1987.

[22] A. De Luca, "Dynamic control of robots with joint elasticity," *Proc. 1988 IEEE Int. Conf. on Robotics and Automation* (Philadelphia, PA, Apr. 24-29, 1988), pp. 152-158.

[23] S. Nicosia, P. Tomei, and A. Tornambè, "Dynamic modelling of flexible robot manipulators," *Proc. 1986 IEEE Int. Conf. on Robotics and Automation*, (San Francisco, CA, Apr. 7-10, 1986), pp. 365-372.

[24] R.H. Cannon, Jr. and E. Schmitz, "Initial experiments on the end-point control of a flexible one-link robot," *Int. J. of Robotics Research*, vol. 3, no. 3, pp. 62-75, 1984.

[25] A. De Luca, P. Lucibello, and G. Ulivi, "Inversion techniques for trajectory control of flexible robot arms," *J. of Robotic Systems*, vol. 6, no. 4, pp. 325-344, 1989.

[26] A. De Luca, L. Lanari, and G. Ulivi, "Nonlinear regulation of end-effector motion for a flexible robot arm," in *New Trends in Systems Theory*, G. Conte, A.M. Perdon, B. Wyman Eds., Birkhäuser, Boston, to appear.

[27] E. Bayo, "A finite-element approach to control the end-point motion of a single-link flexible robot," *J. of Robotic Systems*, vol. 4, no. 1, pp. 63-75, 1985.

Alessandro De Luca
Dipartimento di Informatica e Sistemistica
Università degli Studi di Roma "La Sapienza"
Via Eudossiana 18, 00184 Roma, Italy